Entanglement Hamiltonian of the quantum Néel state

Didier Poilblanc[1]

[1] *Laboratoire de Physique Théorique, CNRS, UMR 5152 and Université de Toulouse, UPS, F-31062 Toulouse, France*

(Dated: September 8, 2014)

Two-dimensional Projected Entangled Pair States (PEPS) provide a unique framework giving access to detailed entanglement features of correlated (spin or electronic) systems. For a bi-partitioned quantum system, it has been argued that the Entanglement Spectrum (ES) is in a one-to-one correspondence with the physical edge spectrum on the cut and that the structure of the corresponding Entanglement Hamiltonian (EH) reflects closely bulk properties (finite correlation length, criticality, topological order, etc...). However, entanglement properties of systems with spontaneously broken continuous symmetry are still not fully understood. The spin-1/2 square lattice Heisenberg antiferromagnet provides a simple example showing spontaneous breaking of SU(2) symmetry down to U(1). The ground state can be viewed as a "quantum Néel state" where the classical (Néel) staggered magnetization is reduced by quantum fluctuations. Here I consider the (critical) Resonating Valence Bond state doped with spinons to describe such a state, that enables to use the associated PEPS representation (with virtual bond dimension $D = 3$) to compute the EH and the ES for a partition of an (infinite) cylinder. In particular, I find that the EH is (almost exactly) a chain of a dilute mixture of heavy (↓ spins) and light (↑ spins) hardcore bosons, where light particles are subject to long-range hoppings. The corresponding ES shows drastic differences with the typical ES obtained previously for ground states with restored SU(2)-symmetry (on finite systems).

arXiv:1407.3830v2 [cond-mat.str-el] 5 Sep 2014

I. INTRODUCTION

It is known from early Quantum Monte Carlo (QMC) simulations that the ground state (GS) of the spin-1/2 Heisenberg antiferromagnet (AFM) on the bipartite square lattice is magnetically ordered [1] and, hence, breaks the hamiltonian SU(2) symmetry. The GS can be viewed as a "quantum Néel state" (QNS) where the maximum classical value $m_{\rm stag} = 1/2$ of the staggered magnetization is reduced by (moderate) quantum fluctuations. More recent QMC simulations [2] have provided GS energy, staggered magnetization and spin-spin correlations with unprecedented accuracy. In particular, it has been established that the QNS exhibits power-law decaying spin-spin correlations characteristic of a *critical state* [3].

Recently, a number of new powerful tools based on entanglement measures have emerged. The entanglement spectrum (ES) and its associated Entanglement Hamiltonian defined via the reduced density matrix (RDM) of a bi-partioned quantum system (see definitions later) provides new insights. In particular, it has been argued that the ES is in a one-to-one correspondence with the physical edge spectrum on the cut for topological ground states [4] and low-dimensional quantum antiferromagnets [5] and that the structure of the corresponding Entanglement Hamiltonian (EH) reflects closely the bulk properties (holographic principle) [6]. However, new interesting features might arise in the entanglement properties of systems with spontaneously broken continuous symmetry, such as the QNS for which SU(2) symmetry is broken down to U(1). First, the entanglement entropy (the entropy associated to the RDM) have revealed anomalous additive (logarithmic) corrections [7, 8] to the area law – i.e. the linear (asymptotic) scaling of the entropy with the length of the cut. It was proposed afterwards that the origin of such corrections may lie in the existence of Goldstone modes [9] associated to the spontaneously broken continuous symmetry. Note however that, in any finite system (as in most "exact" simulations), the SU(2) symmetry is restored by quantum fluctuations and one has a unique GS instead of a degenerate manifold. In fact, recent state-of-the-art SU(2)-symmetric Density Matrix Renormalization Group (DMRG) studies established an interesting correspondence [10], in the (singlet) ground state of two-dimensional antiferromagnets in their magnetically-ordered phases, between the SU(2) tower of states and the lower part of the ES below an "entanglement gap" (although DMRG does not provide information on the momenta of the ES). This suggests strongly that the above-mentioned corrections in the entropy should be associated with the tower of states structure, while the area law arises from ES levels above the entanglement gap [10]. *A priori* important differences may occur in the entanglement properties of a Néel-like wave-function breaking the continuous SU(2) symmetry explicitly i.e. with a finite staggered magnetization. In particular, one expects the ES (and the EH) of a symmetry-broken QNS to differ qualitatively from the ones associated to the GS with restored SU(2) symmetry, computed on finite systems [10, 11]. Computing the entanglement properties of a (variational) state with a finite order parameter is the main goal of this paper.

The formalism of Projected Entangled Pair States (PEPS) [6, 12] enables i) to easily construct symmetry broken variational states and ii) to compute the corresponding EH. Note that, for a given variational state and system size (one uses infinite cylinders with a finite perimeter), the calculation of the EH is *fundamentally exact* and provides a complete analytic expansion in terms of N-body interactions whose amplitudes are numerically

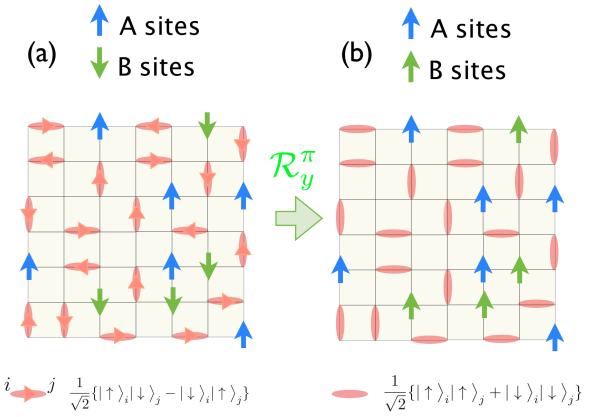

FIG. 1. (a) The Néel state is represented as a spinon-doped RVB state : Singlets are oriented from the A to the B sublattice and doped spinons are polarized along $\hat{z}$ ($-\hat{z}$) on the A (B) sites. Implicitly, a sum over all singlet/spinon configurations is assumed, the average spinon density being controlled by a fugacity. (b) Under a π-rotation around $\hat{y}$ on all the B-sites, all spinons become oriented along $\hat{z}$ and singlets transform into $\frac{1}{\sqrt{2}}\{|\uparrow\uparrow\rangle + |\downarrow\downarrow\rangle\}$ on every NN bonds.

computed. Here I therefore make use of a simple PEPS ansatz of the QNS in order to calculate its EH associated to a bi-partition of an infinite cylinder. The variational wave function used here is in fact the simplest PEPS (i.e. with the smallest bond dimension $D = 3$) one can construct to capture the physics of the symmetry-broken Néel state. Ansätze with a larger bond dimension will not allow to consider a cylinder with a large enough perimeter. Note that the PEPS formalism provides also the momentum-resolved ES. This is to be contrasted to DMRG that also gives easily the ES but without the corresponding momenta of the Schmidt states. Also an analytic form of the EH cannot be obtained in DMRG.

As shown recently using PEPS, a EH with local interactions is expected in a gapped bulk phase (with short-range entanglement), whereas a diverging interaction length of the EH is the hallmark of critical behavior in the bulk [6]. One therefore expects to see fingerprints of the critical behavior of the QNS in its Entanglement Hamiltonian.

II. DOPED-RVB ANSATZ FOR THE NÉEL STATE

I start with the square lattice Resonating Valence Bond (RVB) wavefunction defined as an equal-weight superposition of nearest-neighbor (NN) hardcore singlet coverings [13, 14]. The sign structure of the wave function is fixed by imposing that the singlets $|\uparrow\downarrow\rangle - |\downarrow\uparrow\rangle$ are all oriented from one A sublattice to the other B sublattice. Such a wave function is a global spin singlet – i.e. a SU(2)-invariant state – with algebraic (i.e. critical) dimer correlations (and short-range spin correlations) [15, 16].

To construct a simple ansatz for the QNS, let us now assume that one breaks SU(2) symmetry down to U(1) by doping the NN RVB state with on-site spinons (i.e. spin-1/2 excitations) with *opposite* orientations on the two sublattices. For simplicity, I choose hereafter the staggered magnetization pointing along the $\hat{z}$-axis. Such a simple ansatz is schematically shown in Fig. 1(a). The average density of spinons – identical on the two sublattices – directly gives the staggered magnetization $m_{\rm stag}$ ($\times 2$) and, as one will see later on, can be controlled by a fugacity γ.

Before going further, it is convenient to rewrite the Néel-RVB state in a translationally invariant form. Indeed, under a (spin) π-rotation around $\hat{y}$ on the B-sites, B-spinons transform as $|\downarrow\rangle \to |\uparrow\rangle$ and $|\uparrow\rangle \to -|\downarrow\rangle$. Under such a (unitary) transformation, the new Néel-RVB state acquires the same (average) polarization on the A and B sublattices as shown in Fig. 1(b). The original NN singlets are also transformed into $\frac{1}{\sqrt{2}}\{|\uparrow\uparrow\rangle + |\downarrow\downarrow\rangle\}$ dimers which are now symmetric w.r.t. the bond centers.

III. PEPS CONSTRUCTION AND ENERGETICS

Such a state can in fact be represented by a PEPS $|\Psi_{\rm PEPS}\rangle$ with bond dimension $D = 3$, where each lattice site is replaced by a rank-5 tensor $\mathcal{A}^s_{\alpha,\alpha';\beta,\beta'}$ labeled by one physical index, $s = 0$ or 1, and by four virtual bond indices (varying from 0 to 2) along the horizontal (α, α') and vertical (β, β') directions, as shown in Fig. 2(a). Physically, the absence of singlet on a bond is encoded by the virtual index being "2" on that bond. I define :

$$\mathcal{A} = \mathcal{R} + \gamma \mathcal{S}\,, \tag{1}$$

where $\mathcal{R}$ is the original RVB tensor [17, 18], $\mathcal{S}$ is a polarized spinon tensor and $\gamma \in \mathbb{R}$ is a fugacity controlling the average spinon density. To enforce the hardcore dimer constraint, one takes $\mathcal{R}^s_{\alpha,\alpha';\beta,\beta'} = 1$ whenever three virtual indices equal 2 and the fourth one equals s, and $\mathcal{R}^s_{\alpha,\alpha';\beta,\beta'} = 0$ otherwise. The spinon tensor has only one non-zero element, $\mathcal{S}^1_{2,2;2,2} = 1$. The wave function amplitudes are then obtained by contracting all virtual indices (except the ones at the boundary of the system). Note that the above PEPS ansatz for the Néel state bares similarities with the one used to describe the honeycomb RVB spin liquid under an applied magnetic field [19]. However, a crutial difference is that this new ansatz is, by construction, fully U(1)-invariant in contrast to the spinon-doped RVB state of Ref. [19].

Following a usual procedure, I now place the square lattice of tensors on infinite cylinders with N_v sites in the periodic (vertical) direction as shown in Fig. 2(b) and use standard techniques (involving exact tensor contractions and iterations of the transfer operator) to compute relevant observables. In the PEPS formulation the boundary

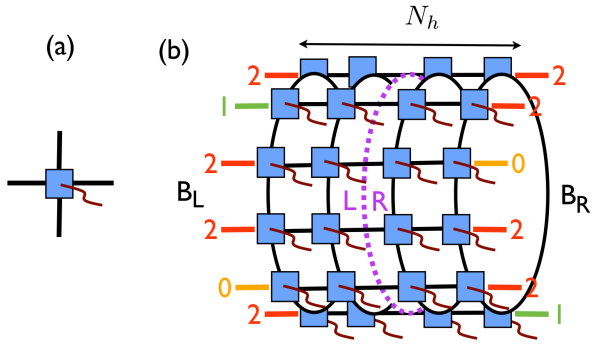

FIG. 2. (Color online) (a) Local (rank-5) PEPS tensor. (b) Tensors are placed on a square lattice wrapped on a cylinder of perimeter N_v and (quasi-) infinite length $N_h \gg N_v$. B_L and B_R boundary conditions are realized by fixing the virtual variables going out of the cylinder ends. A bipartition of the cylinder generates two L and R edges along the cut.

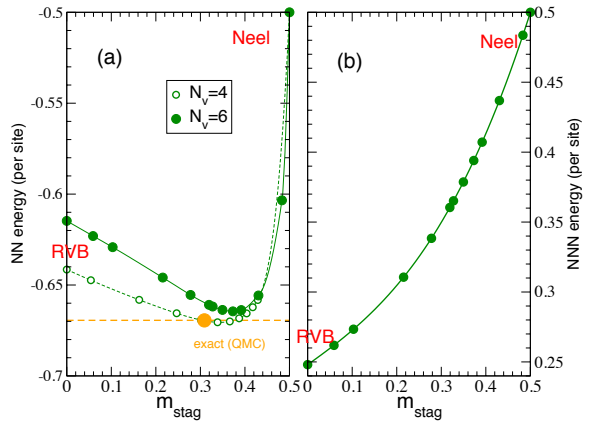

FIG. 3. (Color online) NN (a) and next-NN (b) correlators $2\langle \mathbf{S}_i \cdot \mathbf{S}_j \rangle$ – corresponding to the energies per site in units of the coupling constants – plotted as a function of $m_{\rm stag}$. Computations are done on infinite cylinders of perimeter $N_v = 4$ and $N_v = 6$.

conditions B_L and B_R can be simply set by fixing the virtual states on the bonds "sticking out" at each cylinder end. E.g. open boundary conditions are obtained by setting the boundary virtual indices to "2". Generalized boundary conditions can be realized as in Fig. 2(b) by setting some of the virtual indices on the ends to "0" or "1".

I have computed the (staggered) magnetization $m_{\rm stag}$ and the expectation values of the spin-1/2 Heisenberg exchange interactions $\mathbf{S}_i \cdot \mathbf{S}_j$ between NN and next-NN sites, varying γ from zero to large values (to approach the classical Néel state). The data (normalized as the energy per site of the corresponding Heisenberg model) are displayed as a function of $m_{\rm stag}$ in Fig. 3(a,b). The NN energy shows a broad minimum around $m_{\rm stag} \sim 0.35$, a value a bit larger than the QMC extrapolation ~ 0.307 [2] for the pure NN quantum AFM. However, (i) the variational energy curve is rather flat around the minimum and (ii) the minimum energy is only within $\sim 1.5\%$ of the QMC estimate, a remarkable result considering the simplicity of the one-dimensional family of $D = 3$ PEPS. Note also that the minimum energy agrees very well with optimized $D = 3$ iPEPS [21] and finite PEPS up to $D = 6$ [22].

For completeness, I also show the next-NN energy in Fig. 3(b). In fact, the pure (critical) RVB state provides the lowest next-NN exchange energy, suggesting the existence of a transition, upon increasing the next-NN coupling, from the Néel state to a *gapless* spin liquid [23, 24]. Note that a direct transition from the Néel state to a Valence Bond Crystal – with no intermediate gapless spin liquid phase – is also a realistic scenario [3, 25].

IV. ENTANGLEMENT HAMILTONIAN ON INFINITE CYLINDERS

A. Bipartition and reduced density matrix

To define an Entanglement Hamiltonian associated to the family of Néel-RVB wavefunctions, I partition the $N_v \times N_h$ cylinder into two half-cylinders of lengths $N_h/2$, as depicted in Fig. 2(b). Partitioning the cylinder into two half-cylinders reveals two edges L and R along the cut. Ultimately, I aim to take the limit of infinite Néel-RVB cylinders, i.e. $N_h \to \infty$ as before.

The reduced density matrix of the left half-cylinder obtained by tracing over the degrees of freedom of the right half-cylinder, $\rho_L = {\rm Tr}_R\{|\Psi_{\rm PEPS}\rangle\langle\Psi_{\rm PEPS}|\}$, can be simply mapped, via a spectrum conserving isometry U, onto an operator σ_b^2 acting only on the $D^{\otimes N_v}$ edge (virtual) degrees of freedom, i.e. $\rho_L = U^\dagger \sigma_b^2 U$ [6]. The *Entanglement (or boundary) Hamiltonian* H_b introduced above is defined as $\sigma_b^2 = \exp(-H_b)$. As σ_b^2, H_b is one-dimensional and its spectrum – the *entanglement spectrum* (ES) – is the same as the one of $-\ln \rho_A$. Note that the left and the right half-cylinders give identical EH. For further details on the derivation and the procedure, the reader is kindly asked to refer to Ref. 6.

For a topological state, such as the $\gamma = 0$ RVB state, the Entanglement Hamiltonian depends on the choice of the B_L and B_R cylinder boundaries that define "topological sectors" [18, 20]. Adding any staggered magnetization $m_{\rm stag}$ in the PEPS immediately breaks the gauge symmetry of the tensors which is responsible for the disconnected topological sectors, as also happens in the case of field-induced magnetized RVB states [19]. Therefore, all topological sectors are mixed and H_b become independent of the boundary conditions B_L and B_R provided $N_h \to \infty$. Note also that H_b inherits the U(1) symmetry (associated to rotations around the direction of $m_{\rm stag}$) of the Néel state.

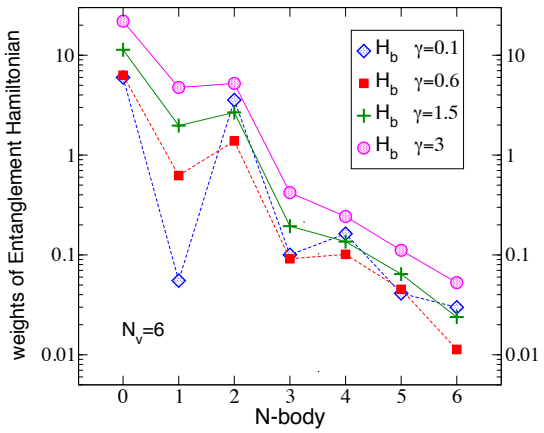

FIG. 4. (Color online) Weights of the Entanglement Hamiltonian H_b expended in terms of N-body operators. Data of several Néel-RVB wavefunctions (whose γ values are mentioned on the plot) are shown. Calculations are done on an infinite cylinder with perimeter $N_v = 6$. As seen e.g. in Ref. [18], finite size effects for such integrated quantities are typically quite small.

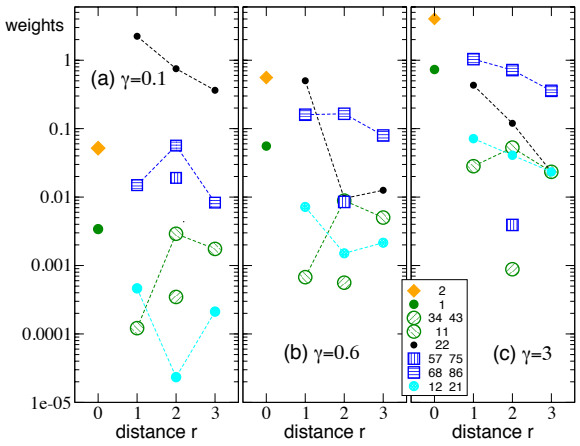

FIG. 5. Largest weights $|c_\nu|$ and $|d_{\nu\mu}(r)|^2$ of the one-body (i.e. $r = 0$) and two-body operators in the expansion of H_b of the Néel-RVB PEPS as a function of distance r, for increasing γ values (corresponding to staggered magnetizations $m_{\rm stag} \sim 0.059, 0.327$ and 0.483, respectively).

B. Expansion in terms of N-body operators

To have a better insight of the Entanglement Hamiltonian, I expand it in terms of a basis of N-body operators, $N = 0, 1, 2, \cdots$ [6, 18]. For this purpose, I use a local basis of $D^2 = 9$ (normalized) $\hat{x}_\nu$ operators, $\nu = 0, \cdots, 8$ which act on the local (i.e. at some site i) configurations $\{|0\rangle, |1\rangle, |2\rangle\}$, where $|2\rangle$ is the vacuum or "hole" state and $|0\rangle$ and $|1\rangle$ can be viewed as spin down and spin up particles, respectively. More precisely, $\hat{x}_0 = \mathbb{I}^{\otimes 3}$, $\hat{x}_1 = \sqrt{\frac{3}{2}}(|0\rangle\langle 0| - |1\rangle\langle 1|)$ and $\hat{x}_2 = \frac{1}{\sqrt{2}}(|0\rangle\langle 0| + |1\rangle\langle 1| - 2|2\rangle\langle 2|)$, for the diagonal matrices, complemented by $\hat{x}_3 = \hat{x}_4^\dagger = \sqrt{3}|0\rangle\langle 1|$ acting as (effective) spin-1/2 lowering/raising operators, and $\hat{x}_5 = \hat{x}_7^\dagger = \sqrt{3}|2\rangle\langle 0|$ and $\hat{x}_6 = \hat{x}_8^\dagger = \sqrt{3}|2\rangle\langle 1|$ acting as particle hoppings. In this basis H_b reads [18],

$$H_b = c_0 N_v + \sum_{\nu,i} c_\nu \hat{x}_\nu^i + \sum_{\nu,\mu,r,i} d_{\nu\mu}(r)\, \hat{x}_\nu^i \hat{x}_\mu^{i+r} + \sum_{\lambda,\mu,\nu,r,r',i} e_{\lambda\mu\nu}(r,r')\, \hat{x}_\lambda^i \hat{x}_\mu^{i+r} \hat{x}_\nu^{i+r'} + \cdots , \quad (2)$$

where site superscript indices have been added and only the first one-body, two-body and three-body terms are shown.

The total weights corresponding to each order of the expansion of H_b in terms of N-body operators are shown in Fig. 4 as a function of the order N using a semi-logarithmic scale. The data reveal clearly a fast decay of the weight with the order N. This decay is compatible with an exponential law although more decades in the variation of the weights (i.e. larger N_v) would be needed to draw a definite conclusion. In any case, H_b is dominated by two-body contributions in addition to the normalization constant and subleading one-body terms. The quantum Néel state is believed to be critical with power-law decay of spin-spin correlations [3]. Therefore, according to Ref. [6], one expects H_b to be long-ranged to some degree. So, one still needs to refine the analysis and investigate further the r-dependence of the leading two-body contributions. In the next Subsection, I show that H_b indeed possesses long-range two-body terms that I characterize.

C. Entanglement Hamiltonian: an effective one-dimensional t–J model

It is known that the EH of the $\gamma = 0$ RVB PEPS belongs to the $1/2 \oplus 0$ representation of SU(2) and its Hilbert space is the same as the one of a one-dimensional bosonic t–J model [18], interpreting $|0\rangle$ and $|1\rangle$ states ($|2\rangle$ states) as $\downarrow$ and $\uparrow$ spins (holes). In the presence of a finite (staggered) magnetization in the bulk, the SU(2) symmetry is broken but H_b keeps the unbroken $U(1)$ symmetry corresponding to spin rotations around the direction of the staggered magnetization.

The (largest) non-zero real coefficients in (2) computed on an infinitely-long cylinder of perimeter $N_v = 6$ are shown in Fig. 5(a-c) for small (a), intermediate (b) and large (c) (staggered) magnetizations. At large and intermediate values of $m_{\rm stag}$, one finds a dominant one-body (diagonal) term which can be interpreted as a chemical potential term (up to a multiplicative factor) :

$$\mathcal{H}_2 = c_2 \sum_i \hat{x}_2^i = \frac{3}{\sqrt{2}} c_2 \sum_i (n_i - 2/3)\,, \quad (3)$$

where n_i counts the number of particles (i.e. "0" and "1" states) on site i. The subleading one-body operator takes the form of a Zeeman coupling :

$$\mathcal{H}_1 = \sqrt{6} c_1 \sum_i S_i^z \,, \tag{4}$$

where S_i^z is an effective spin-1/2 component (along $\hat{z}$) and $c_1 \simeq c_2/10$.

The leading 2-body contributions are hopping terms *at all distances* for the majority "spins" ($|1\rangle$ states) :

$$\begin{aligned} \mathcal{H}_{68}(r) &= d_{68}(r) \sum_i (\hat{x}_8^i \hat{x}_6^{i+r} + \hat{x}_6^i \hat{x}_8^{i+r}) \\ &= 3 d_{68}(r) \sum_i (b_{i+r,1}^\dagger b_{i,1} + b_{i,1}^\dagger b_{i+r,1}) \,, \end{aligned} \tag{5}$$

where $b_{i,s}^\dagger$ ($b_{i,s}$) are the canonical bosonic creation (annihilation) operators of the virtual $s = 0, 1$ states. Note that the minority spins ($|0\rangle$ states) only hop at *even* distances (weights at odd distances are negligable) with much weaker amplitudes, $d_{57} = d_{75} \ll d_{68} = d_{86}$. The next subleasing corrections are diagonal 2-body density-density interactions

$$\begin{aligned} \mathcal{H}_{22}(r) &= d_{22}(r) \sum_i \hat{x}_2^i \hat{x}_2^{i+r} \\ &= \frac{9}{2} d_{22}(r) \sum_i (n_i - 2/3)(n_{i+r} - 2/3) \,, \end{aligned} \tag{6}$$

which become dominant when $\gamma, m_{\rm stag} \to 0$.

Other generic operators allowed by the $U(1)$ symmetry, like the anisotropic XXZ chain ($d_{11} \neq d_{34} = d_{43}$) or mixed operators of the form $\mathcal{H}_{12} \propto \sum_i S_i^z (n_{i\pm r} - 2/3)$ are also present but their amplitudes turn out to be quite small. Interestingly, H_b (approximately) conserves the hole "2-charge" and, hence, does not contain pair-field operators with sizable amplitudes, in contrast to previous studies of $D = 3$ PEPS [18, 19]. If one restricts to the dominant contributions (3) and (5), H_b is exactly a chain of a dilute mixture of heavy ($\downarrow$ spins or $|0\rangle$ states) and light ($\uparrow$ spins or $|1\rangle$ states) hardcore bosons, where light particles are subject to long-range hopping.

V. ENTANGLEMENT SPECTRUM

It is also of high interest to examine the ES in the QNS and compare it to ES obtained for GS where SU(2)-symmetry is restored on finite size systems [10]. By definition the ES is the spectrum of $-\ln \rho_L$. Since ρ_L and $\sigma_b^2 = \exp(-H_b)$ are related by an isometry, it is also the spectrum of the Entanglement Hamiltonian H_b. ES are shown in Fig. 6(a-c) for 3 values of the fugacity γ, as a function of the momentum along the cut. Since σ_b^2 conserves the total S_z of the chain ($U(1)$ symmetry), it can be block-diagonalized using this quantum number and the eigenvalues of $-\ln \sigma_b^2$ are displayed in each S_z sector separately. It can be seen from Fig. 6(a) that

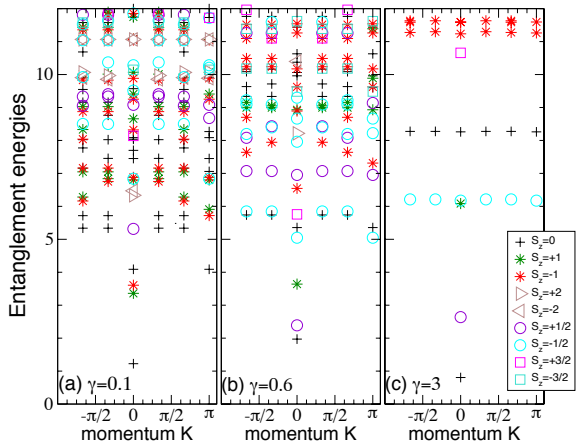

FIG. 6. Entanglement spectrum of a bipartitioned $N_v = 6$ RVB-Néel cylinder as a function of the momentum along the cut, for different values of the spinon fugacity $\gamma = 0.1, 0.6$ and 3 corresponding to $m_{\rm stag} \sim 0.059, 0.327$ and 0.483, respectively. Different symbols are used for different S_z sectors of the edge.

the $\gamma = 0$ SU(2) spin multiplets are split by a small spinon density. For increasing γ (i.e. staggered magnetization), the splittings of the Kramer's multiplets increase (see Fig. 6(b,c)) due to the relative increase of the amplitudes of the SU(2)-symmetry breaking terms like (5) in the EH. In the limit of large γ where the classical Néel state is approached, one finds separated bands of energy levels. It may be that the ES is gapped for all γ but finite size effects remain too large to reach a definite conclusion. In any case, the ES of Fig. 6 are to be contrasted to the ES obtained in DMRG for GS with restored SU(2)-symmetry (due to the use of finite size systems). Obviously the two types of ES are very different with a SU(2) tower of states structure at low energy for the ES of the singlet GS [10] and a U(1) symmetric ES in the (variational) symmetry-broken Néel state.

VI. SUMMARY AND DISCUSSION

In this paper, I have investigated entanglement properties of a simple one-dimensional family of PEPS designed to describe qualitatively the GS of the square lattice AFM. These ansätze exhibit a finite staggered magnetization i.e. they break explicitly the SU(2) symmetry down to U(1) and can be studied on infinite cylinders with a finite perimeter. The goal of this study is therefore to examine the effects of such a finite order parameter on various entanglement properties and compare them to (QMC or SU(2)-symmetric DMRG) studies where symmetry is restored in a finite system. Thanks to the PEPS structure, the Entanglement Hamiltonian associated to a bipartition of the cylinder can be derived exactly (for a fixed perimeter). It is found that the EH inherits the

U(1) symmetry of the Néel state and possesses a very simple structure : (i) its Hilbert space is the same as the one of a one-dimensional bosonic t–J model, interpreting the 3 virtual states on the edge as a $\uparrow$ spin, a $\downarrow$ spin and a hole, (ii) when expended using a local basis of operators, it shows dominant two-body interactions and (iii) higher-order operators (three-body terms and beyond) represent less than 10% of its total weight. Examining in details the form of the two-body interactions, I find that the dominant ones are long-range hoppings of the majority (let say $\uparrow$) spins. It is however not possible to distinguish a power-law versus an exponential decay of these hopping terms. In any case, the associated Entanglement Spectrum is found to be qualitatively very different from the ones obtained in GS with restored SU(2)-symmetry [10] (no tower of states structure is found, as suspected). Whether the entropy exhibits additive logarithmic corrections as in Refs. [7, 8] is difficult to answer. The absence of the tower of states in the ES suggests a negative answer. However, an hypothetical power-law decay of the hopping terms in the EH (instead of exponential) might lead to some additive corrections to the entropy. It would be interesting to complement our calculation of the ES using "conceptually exact" numerical methods (such as QMC or SU(2)-symmetric DMRG) on large but finite systems, adding a small external staggered field (to produce a finite order parameter), taking the limit of infinite system size first.

I acknowledge fundings by the "Agence Nationale de la Recherche" under grant No. ANR 2010 BLANC 0406-0 and support from the CALMIP supercomputer center (Toulouse). I thank Claire for her patience and I am indebted to Fabien Alet, Ignacio Cirac, Nicolas Laflorencie, Roger Melko, Anders Sandvik, Norbert Schuch and Frank Verstraete for numerous discussions and insightful comments.

[1] J. D. Reger and A. P. Young, *Monte Carlo Simulations of the Spin-1/2 Heisenberg Antiferromagnet on a Square Lattice*, Phys. Rev. B **37**, 5978 (1988).

[2] A. W. Sandvik and H. G. Evertz, *Loop updates for variational and projector quantum Monte Carlo simulations in the valence-bond basis*, Phys. Rev. B **82**, 024407 (2010).

[3] A. W. Sandvik, *Lecture notes for course given at the 14th Training Course in Physics of Strongly Correlated Systems, Salerno (Vietri sul Mare), Italy, in October 2009*, AIP Conf.Proc. 1297:135 (2010).

[4] Hui Li and F. D. M. Haldane, *Entanglement Spectrum as a Generalization of Entanglement Entropy: Identification of Topological Order in Non-Abelian Fractional Quantum Hall Effect States*, Phys. Rev. Lett. **101**, 010504 (2008).

[5] Didier Poilblanc, *Entanglement spectra of quantum Heisenberg ladders*, Phys. Rev. Lett. **105**, 077202 (2010).

[6] J. I. Cirac, D. Poilblanc, N. Schuch, and F. Verstraete, *Entanglement spectrum and boundary theories with projected entangled-pair states*, Phys. Rev. B **83**, 245134 (2011).

[7] A. B. Kallin, M. B. Hastings, R. G. Melko, and R. R. P. Singh, *Anomalies in the entanglement properties of the square-lattice Heisenberg model*, Phys. Rev. B **84**, 165134 (2011).

[8] Hyejin Ju, A. B. Kallin, P. Fendley, M. B. Hastings, and R. G. Melko, *Entanglement scaling in two-dimensional gapless systems*, Phys. Rev. B **85**, 165121 (2012).

[9] M. A. Metlitski and T. Grover, *Entanglement Entropy of Systems with Spontaneously Broken Continuous Symmetry*, arXiv:1112.5166 (2011).

[10] F. Kolley, S. Depenbrock, I.P. McCulloch, U. Schollwöck, and V. Alba, *Entanglement spectroscopy of SU(2)-broken phases in two dimensions*, Phys. Rev. B **88**, 144426 (2013).

[11] D. J. Luitz, N. Laflorencie, and F. Alet, *Participation spectroscopy and entanglement Hamiltonian of quantum spin models*, arXiv:1404.3717 (2014).

[12] N. Schuch, M. M. Wolf, F. Verstraete, and J. I. Cirac, *Computational Complexity of Projected Entangled Pair States*, Phys. Rev. Lett. **98**, 140506 (2007).

[13] P. W. Anderson, *Resonating valence bonds: A new kind of insulator?*, Mat. Res. Bull. **8**, 153 (1973).

[14] P. W. Anderson, *The resonating valence bond state in La_2CuO_4 and superconductivity*, Science **235**, 1196 (1987).

[15] A. F. Albuquerque and F. Alet, *Critical correlations for short-range valence-bond wavefunctions on the square lattice*, Phys. Rev. B **82**, 180408R (2010).

[16] Y. Tang, A. W. Sandvik and C. L. Henley, *Properties of resonating valence bond spin liquids and critical dimer models*, Phys. Rev. B **84**, 174427 (2011).

[17] N. Schuch, D. Poilblanc, J. I. Cirac and D. Perez-Garcia, *Resonating valence bond states in the PEPS formalism*, Phys. Rev. B **86**, 115108 (2012).

[18] D. Poilblanc, N. Schuch, D. Perez-Garcia and J. I. Cirac, *Topological and entanglement properties of resonating valence bond wave functions*, Phys. Rev. B **86**, 014404 (2012).

[19] D. Poilblanc, N. Schuch, and J. I. Cirac, *Field-induced superfluids and Bose liquids in Projected Entangled Pair States*, Phys. Rev. B **88**, 144414 (2013).

[20] N. Schuch, D. Poilblanc, J. I. Cirac and D. Perez-Garcia, *Topological order in PEPS: Transfer operator and boundary Hamiltonians*, Phys. Rev. Lett. **111**, 090501 (2012).

[21] Bela Bauer, Guifre Vidal, and Matthias Troyer, *Assessing the accuracy of projected entangled-pair states on infinite lattices*, J. Stat. Mech (2009) P09006.

[22] M. Lubasch, J. I. Cirac, and M.-C. Bañuls, *Algorithms for finite Projected Entangled Pair States*, arXiv:1405.3259 (2014).

[23] Ling Wang, Didier Poilblanc, Zheng-Cheng Gu Xiao-Gang Wen and Frank Verstraete, *Constructing gapless spin liquid state for the spin-1/2 J1-J2 Heisenberg model on a square lattice*, Phys. Rev. Lett. **111**, 037202 (2013).

[24] Shou-Shu Gong, Whei Zhu, D. N. Sheng Olexei I. Motrunich and Matthew P. A. Fisher, *Plaquette Ordered Phase and Quantum Phase Diagram in the Spin-1/2 J1-J2 Square Heisenberg Model*, Phys. Rev. Lett. **113**, 027201 (2013).

[25] H.J. Schulz, T. Ziman and D. Poilblanc, *Magnetic order*

and disorder in the J1J2 model, J. Phys. I France **6**, 675-703 (1996).